

# Auto-ignition Characteristics of Gasoline and Diesel Fuel Blends: A High-Pressure Ignition Delay and Kinetic Modelling Study

Yang Li<sup>\*,1,2</sup>

<sup>1</sup>Science and Technology on Combustion, Internal Flow and Thermo-structure Laboratory, School of Astronautics, Northwestern Polytechnical University, Xi'an 710072, China

<sup>2</sup>Clean Combustion Research Centre, King Abdullah University of Science and Technology, Thuwal, Saudi Arabia

## Abstract

The ignition delay times (IDTs) of two different certified gasoline and diesel fuel blends are reported. These measurements were performed in a shock tube and in a rapid compression machine over a wide range of experimental conditions ( $\phi = 0.5 - 2.0$ ,  $T = 700 - 1400$  K and  $p = 10 - 20$  bar) relevant to internal combustion engine operation. In addition, the measured IDTs were compared with two relevant gasoline fuels: Coryton gasoline and Haltermann gasoline systematically under the same experimental conditions. Two different gasoline surrogates a primary reference fuel (PRF) and toluene PRF (TPRF) were formulated, and two different gasoline surrogate models were employed to simulate the experiments. Typical pressure and equivalence ratio effects were obtained, and the reactivity of the four different fuels diverge in the negative temperature coefficient (NTC) regime (700 – 900 K). Particularly at 750 K, the discrepancy is about a factor of 1.5 – 2.0. For the high Research Octane Number (RON) and high-octane sensitivity fuel, the simulation results obtained using the TPRF surrogate was found to be unreasonably slow compared to experimental results, due to the large quantity of toluene (77.6% by volume) present. Further investigation including reactants' concentration profile, flux and sensitivity analyses were simultaneously carried out, from which, toluene chemistry and its interaction with alkane (n-heptane and iso-octane) chemistry were explained in detail.

*Keywords:* Gasoline and diesel; Shock tube; Rapid compression machine; Ignition delay time; Gasoline surrogate

---

\* Corresponding author: [yangli.nuig@gmail.com](mailto:yangli.nuig@gmail.com)

# 汽油和柴油掺混燃料的着火特性：高压下的点火延迟实验和反应动力学模型的研究

李阳<sup>\*1,2</sup>

<sup>1</sup>西北工业大学，航天学院，燃烧、热结构与内流场重点实验室，陕西，西安，710076

<sup>2</sup>阿卜杜拉国王科技大学，清洁燃烧研究中心，图瓦，沙特阿拉伯

## 摘要

研究了两种已经认证的汽油和柴油掺混燃料的点火延迟时间。所有的实验测量都在激波管和快速压缩机中完成，实验条件覆盖了宽泛的发动机工况： $\phi = 0.5 - 2.0$ ， $T = 700 - 1400$  K and  $p = 10 - 20$  bar)。此外，测得的点火延迟时间也同另外两个相关的汽油燃料：Coryton 汽油和 Haltermann 汽油的实验结果做了系统性的对比。两种简单的汽油替组分：正标准参考燃料（PRF）和甲苯标准参考燃料（TPRF），以及两个反应动力学模型被用来模拟预测实验结果。实验结果展示出：1) 对于各个不同的燃料，压力和当量比对点火延迟时间的典型性影响；2) 对于四种不同的燃料，在负温度系数区（700 - 900 K）的反应活性的较大差异。具体定量的来讲，在温度为 750 K 时，两种不同的汽油和柴油掺混燃料的点火延迟时间相差为 1.5 - 2.0 倍。对于高辛烷值和高敏感性的燃料（Coryton 汽油）来说，用甲苯标准参考燃料（TPRF）来模拟的结果显示出非常规的低反应活性，这主要是由于燃料组分中大量的甲苯的存在（77.6%的体积比例）。为了探究此现象背后的反应动力学规律，本文对于甲苯以及甲苯跟烷烃（正庚烷和异辛烷）的相互作用，进行了深入的反应物的浓度消耗曲线，反应通量的分析，以及敏感性分析。

**关键词：**汽油和柴油；激波管；快速压缩机；点火延迟时间；汽油替代组分

**中图分类号：**TJ5

---

\* Corresponding author: [yangli.nuig@gmail.com](mailto:yangli.nuig@gmail.com)

## 1. Introduction

Commercial transportation grade gasoline and diesel are the most widely used light- and heavy-duty transportation fuels and are complex mixtures of hundreds of hydrocarbons including linear and branched paraffins, naphthenes, olefins, and aromatics [1, 2]. The co-optimization of fuel/engine systems requires an in-depth knowledge of the autoignition behavior of the fuel. Particularly for higher efficiency spark ignition engines, knocking of the end-gas is fundamentally related to the fuel's autoignition (combustion kinetics) characteristics [3, 4].

Recently, there have been very limited experimental autoignition measurements of gasoline and/or diesel fuels in shock tubes (ST) and rapid compression machines (RCMs) in the literature. To the best of our knowledge, the only ignition delay time (IDT) measurements of diesel fuel in a RCM were performed by Kukkadapu *et al.* [5], in which the IDT measurements of two well-characterized reference diesel fuels, namely commercial grade ultra-low-sulfur diesel (ULSD#2) and Fuels for Advanced Combustion Engines research diesel (FD9A). The experimental results showed that diesel blends with similar cetane ratings and different compositional makeups exhibited varying ignition propensities over different temperature regimes, thereby demonstrating the effect of molecular composition on autoignition characteristics. In particular the difference in ignition propensities was observed at temperatures at which the low temperature branching reactions are active. We have summarized the literature studies that have focused on autoignition of diesel fuels in Table S1 in the Supplementary Material 1, including the facilities used and the conditions of pressure, temperature, equivalence ratio, and dilution studied in the experiments.

Lee *et al.* [6] investigated the autoignition behavior of two oxygenated certification gasoline fuels: Haltermann Gasoline (RON = 91) and Coryton gasoline (RON = 97.5) in both a high-pressure shock tube and in a rapid compression machine at pressures of 10, 20 and 40 atm, and equivalence ratios of 0.45, 0.9 and 1.8. The experimental results were simulated using three different gasoline surrogate models. It was found that the effects of fuel octane number and fuel composition on ignition characteristics are strongest in the intermediate temperature (negative temperature coefficient) regime.

Also, it was shown that more complex surrogate mixtures are needed to emulate the reactivity of gasoline with higher octane sensitivity ( $S = \text{RON} - \text{MON}$ ).

As a succeeding investigation of the above study from Lee *et al.* [6], the objectives of this study are three\_fold: 1) To investigate the autoignition characteristics of two oxygenated gasoline/diesel fuel blends over a range of pressures (10 – 20 bar), temperatures (700 – 1400 K) and equivalence ratios in a well heated ST and a RCM; 2) To formulate two different gasoline surrogates; a PRF and a TPRF, and simulate the experimental results using two different gasoline surrogate models from Lawrence Livermore National Laboratory (LLNL) [7] and King Abdullah University of Science and Technology (KAUST) [8]; 3) To systematically compare the reactivity of the two gasoline fuels studied by Lee *et al.* [6] and the two gasoline/diesel fuel blends developed in this study.

## 2. Experimental method and conditions

The two certification gasolines/diesel fuel blends used in this study were supplied by Coryton Advanced Fuels, and the fuel compositions were determined using detailed hydrocarbon analysis (DHA) at Saudi Aramco’s Research and Development Center as described by Lee *et al.* [6].

The compositions of Coryton gasoline and diesel were summarized in Table S2 and S3 in the Supplementary Material 1 respectively, using the above detection method. The two Coryton gasoline/diesel fuel blends used in this study were blended using 75/25 and 50/50 (% by volume) gasoline/diesel, respectively, as shown in Table 1.

Table 1. The two Coryton gasoline/diesel fuel blends used in this study.

	Coryton Gasoline/Diesel (75/25)	Coryton Gasoline/Diesel (50/50)
Volume ratio (L %)	75/25	50/50
Mole ratio (mol %)	84/16	64/36
Formula	$\text{C}_{7.49}\text{H}_{13.28}\text{O}_{0.08}$	$\text{C}_{8.81}\text{H}_{15.69}\text{O}_{0.06}$

Table 2 summarized the experimental conditions investigated in this work, notably, experiments of Coryton Gasoline and Haltermann Gasoline were carried in the paper by Lee *et al.* [6]. These are conditions of direct relevance to gasoline, diesel, and low-temperature combustion (LTC) engine technologies. In this way, for each individual fuel, the pressure and equivalence ratio effects on IDT can be systematically evaluated, and at an equivalence ratio of 0.5, 1.0 and a pressure of 10, 20 atm the reactivity can be consistently compared.

Table 2. Experimental conditions of four gasoline and diesel fuels and fuel blends.

Fuel	Coryton Gasoline	Haltermann Gasoline	Coryton Gasoline /Diesel (75/25)	Coryton Gasoline /Diesel (50/50)
10 atm	–	–	✓	✓
$\phi = 0.5$ 20 atm	✓	✓	✓	✓
40 atm	–	–	–	–
10 atm	✓	✓	✓	✓
$\phi = 1.0$ 20 atm	✓	✓	✓	–
40 atm	✓	✓	–	–
10 atm	–	–	✓	–
$\phi = 2.0$ 20 atm	✓	✓	✓	–
40 atm	–	–	–	–
Formula	$C_{6.46}H_{11.39}O_{0.10}$	$C_{6.11}H_{12.07}O_{0.21}$	$C_{7.49}H_{13.28}O_{0.08}$	$C_{8.81}H_{15.69}O_{0.06}$

All experiments were performed in the NUI Galway HPST and RCM facilities as described previously by Lee *et al.* [6]. Detailed uncertainty analysis of the measurements was introduced by Li *et al.* [9]. It is worth nothing that, to perform experiments on these two extreme, low-vapor pressure gasoline/diesel fuel blends, the heating system of the RCM was systematically upgraded, and the initial temperatures of the HPST and RCM were maintained at 120 °C and 150 °C, respectively.

Furthermore, to confirm that these two low-vapor pressure gasoline/diesel fuel blends did vaporize, an optically accessible test cell was constructed to measure the IR absorption coefficients of the fuel mixture at 3.39  $\mu\text{m}$ , and the measurement was carried out on the preheated HPST as well. Using this arrangement, a two-point transmitted light intensity measurement yields the test gas absorption coefficient in accordance with the Beer-Lambert law:

$$A = \log_{10}[I_0/I_T] = \epsilon lc$$

where  $A$  is light absorbance,  $\epsilon$  is the molar absorption coefficient,  $l$  is the optical path length and  $c$  is concentration.  $I_0$  and  $I_T$  are the incident and transmitted light intensities.

Fig 1 shows good agreement between the absorbance measurements as a function of partial pressure for the Coryton gasoline/diesel 75/25 fuel blends injected into the test cell and fuel/air mixture prepared in the HPST. The measurements in the HPST cover the upper limit of total pressure used in the experiments ( $\approx 1500$  mbar), and the molar absorption coefficient  $\epsilon$  for this gasoline/diesel blend has been calculated to be  $9.62 \text{ m}^2 \text{ mol}^{-1}$ .

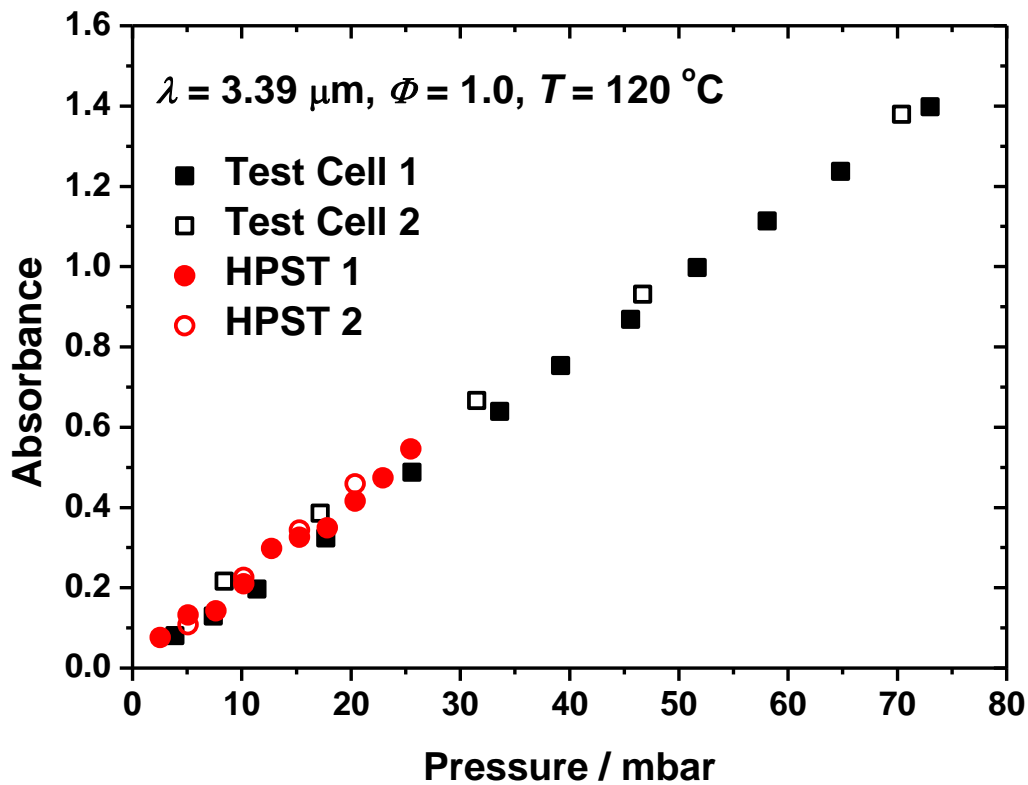


Fig 1. Fuel concentration measurements by 3.39  $\mu\text{m}$  He-Ne laser absorption (Coryton gasoline/diesel 75/25 fuel blends).

In addition, a simple injection test was also performed simultaneously. By injecting 0.5 – 1.0 ml volume of fuel into a vacuumed fuel tank at one time, the pressure was monitored instantly. Figure 2 shows the testing results, in which a linear relation between the monitored pressure and injected volume of fuel was observed, this again testified the complete vaporization of the gasoline and diesel blends.

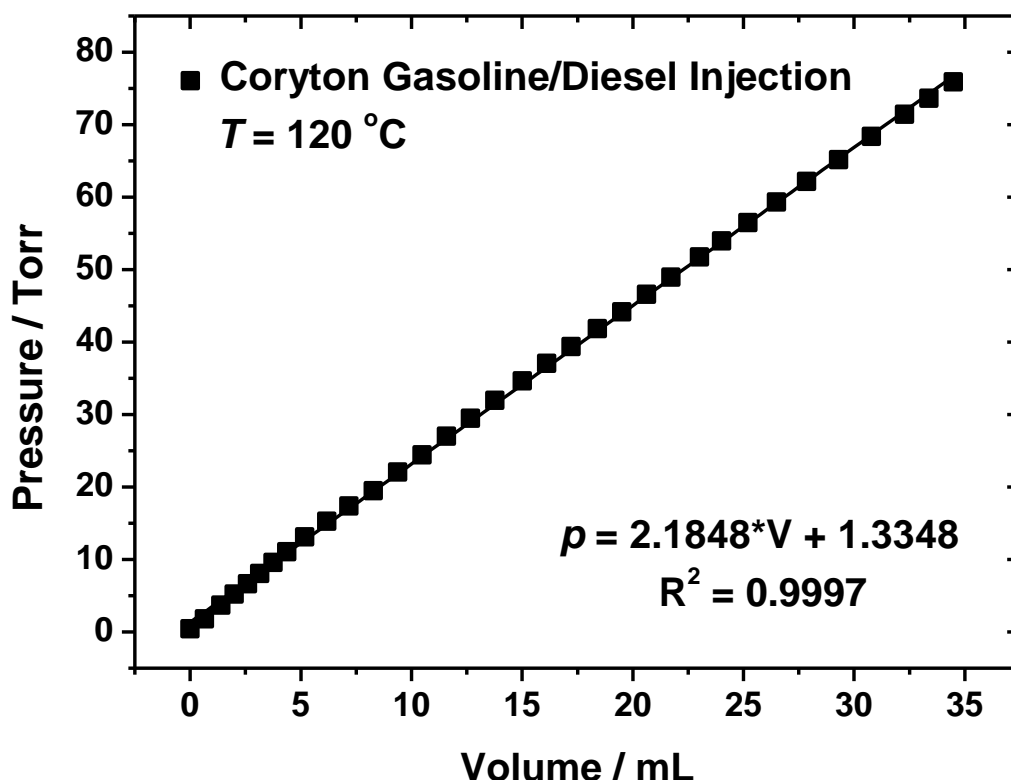


Figure 2. Fuel injection test: monitored pressure as function of injected volume of fuel.

### 3. Surrogate model simulation

Octane number (ON) is an important indicator of the anti-knock quality of commercial gasoline fuels. It is experimentally measured in a Cooperative Fuel Research (CFR) engine under two standard operating procedures: ASTM D2699 [10] and ASTM D2700 [11], resulting in the research octane number (RON) and motor octane number (MON) respectively. Primary reference fuels (PRF) is the simplest surrogate used for representing a real gasoline fuel, which are binary blends of iso-octane and n-heptane. By definition, the RON and MON values assigned for iso-octane and n-heptane are both 100 and 0 respectively. In addition, the difference and average values between the two properties are

defined as octane sensitivity ( $S = \text{RON} - \text{MON}$ ) and anti-knock index ( $\text{AKI} = (\text{RON} + \text{MON}) / 2$ ) respectively. In order to match the octane sensitivity of a commercial fuel, toluene primary reference fuel (TPRF) is another commonly used simple gasoline surrogate, which is a ternary mixture of PRF-components and toluene. Toluene is a highly unsaturated hydrocarbon or aromatic hydrocarbon, with the RON and MON values of 120 and 109 respectively [12].

Table 3 summarized the key properties of investigated in this work and from that of Lee *et al.* [6], which include the research octane number (RON), motor octane number (MON), octane sensitivity and anti-knock index (AKI) values. In general, these properties all decrease as we move from the pure Coryton gasoline fuel to the (50/50) Coryton gasoline/diesel blend. Based on these properties, two different gasoline surrogates (a PRF and a TPRF blend) were formulated by emulating the AKI, RON and octane sensitivity [12, 13], as shown in Table 4.

Table 3 Comparison of the key properties of four different fuels.

Fuel	Coryton Gasoline	Haltermann Gasoline	Coryton Gasoline /Diesel (75/25)	Coryton Gasoline /Diesel (50/50)
RON	97.5	91	80	61
MON	86.6	83.4	73.8	55
Sensitivity	10.9	7.6	6.2	6
AKI	92.05	87.2	76.9	58

Table 4 Gasoline surrogate formulation for four different fuels.

Fuel	Coryton Gasoline		Haltermann Gasoline		Coryton Gasoline /Diesel (75/25)		Coryton Gasoline /Diesel (50/50)	
	PRF	TPRF	PRF	TPRF	PRF	TPRF	PRF	TPRF
iso-Octane	92.05	8.1	87.2	54	76.9	35.46	58	14.52
n-Heptane	17.95	14.3	12.8	17	23.1	29.64	42	51.03
Toluene	–	77.6	–	29	–	34.9	–	34.45

Two different gasoline surrogate models, one from Lawrence Livermore National Laboratory (LLNL) [7] and the other from King Abdullah University of Science and Technology (KAUST) [8], were employed to simulate the experimental data using the two gasoline surrogates formulated above:

- LLNL (1389 species and 5935 reactions)
- KAUST (2768 species and 9236 reactions)

#### 4. Results and Discussion

At  $\phi = 1.0$  and  $p = 10$  atm, the IDTs of the four different fuels are compared, Figure 3. At intermediate to high temperatures (900 – 1400 K), the four fuels have the same reactivity (solid symbols), while in NTC regime (700 – 900 K), IDTs decrease with the pure Coryton fuel having the longest ignition times and the 50/50 Coryton gasoline/diesel fuel having the fastest ignition times (open symbols). Particularly at around 750 K, the IDT differ by about a factor of 2.0 between the two different (75/25 and 50/50) Coryton gasoline/diesel fuel blends.

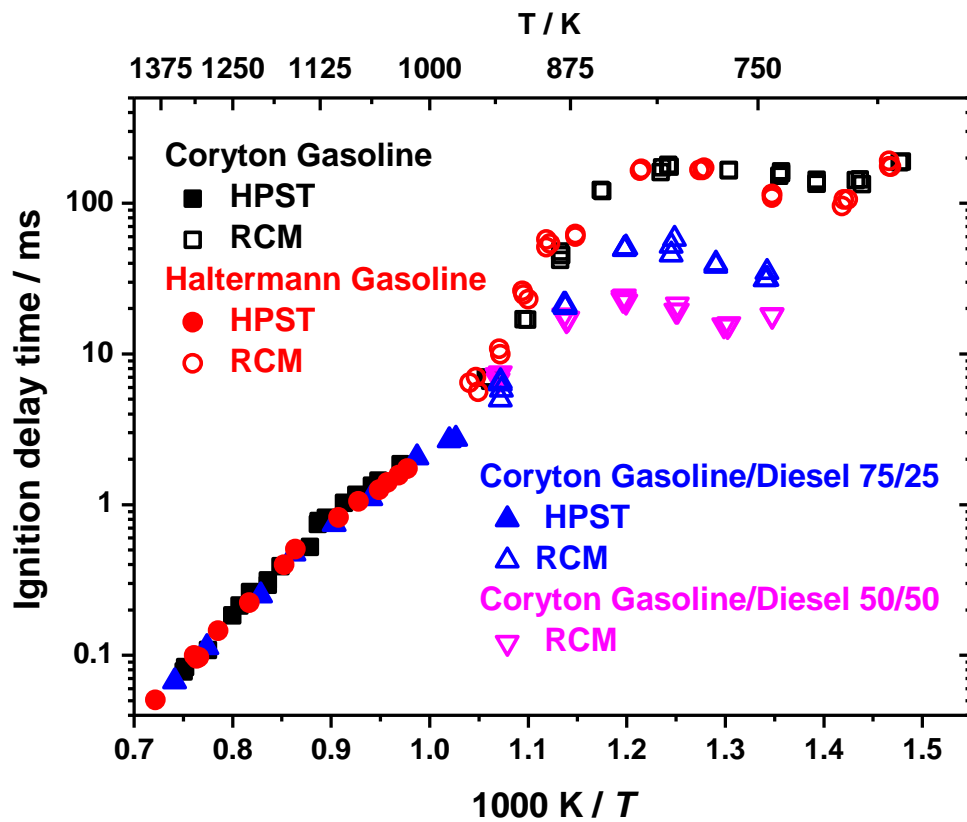


Figure 3. Fuel reactivity comparison at  $\phi = 1.0$  and  $p = 10$  atm.

Figure 4 presents the pressure effect on IDTs for the Coryton gasoline/diesel 75/25 fuel blend for data measured in both the HPST and in the RCM at  $\phi = 1.0$ ,  $p = 10$  and 20 atm. In addition, simulation results generated using KAUST model and two different gasoline surrogates are also systematically compared. Similarly, the equivalence ratio effect on IDTs for the Coryton gasoline/diesel 50/50 fuel blend is shown in Figure 5 for experimental results obtained in the RCM at  $\phi = 0.5$  and 1.0,  $p = 10$  atm. Figure 5 also include simulated ignition times using KAUST model and two different gasoline surrogates. Note, because of the limitation of the length of this paper, the simulation results generated using LLNL model and two different gasoline surrogates were presented and systematically compared in supplementary material. All these simulations have taken the facility effects into account (heat loss of RCM), and the volume-time histories have also been provided as supplementary material.

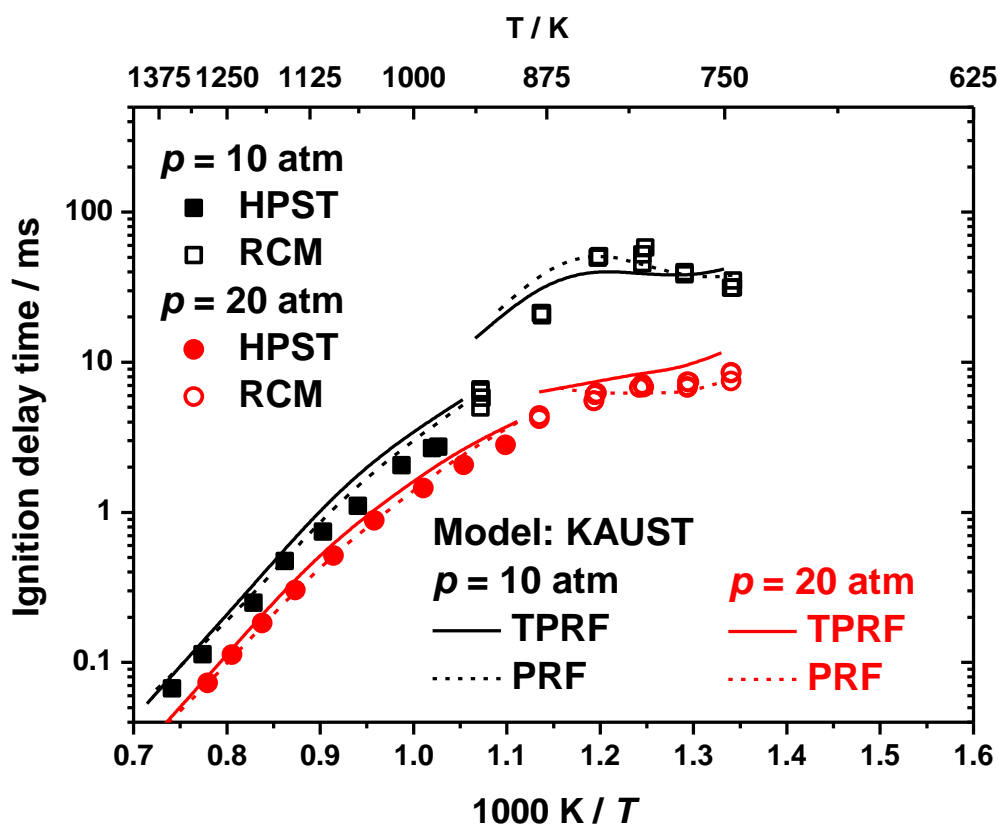


Figure 4. IDT simulation for Coryton gasoline/diesel 75/25 fuel blend using two different gasoline surrogates at  $\phi = 1.0$ ,  $p = 10$  and 20 atm.

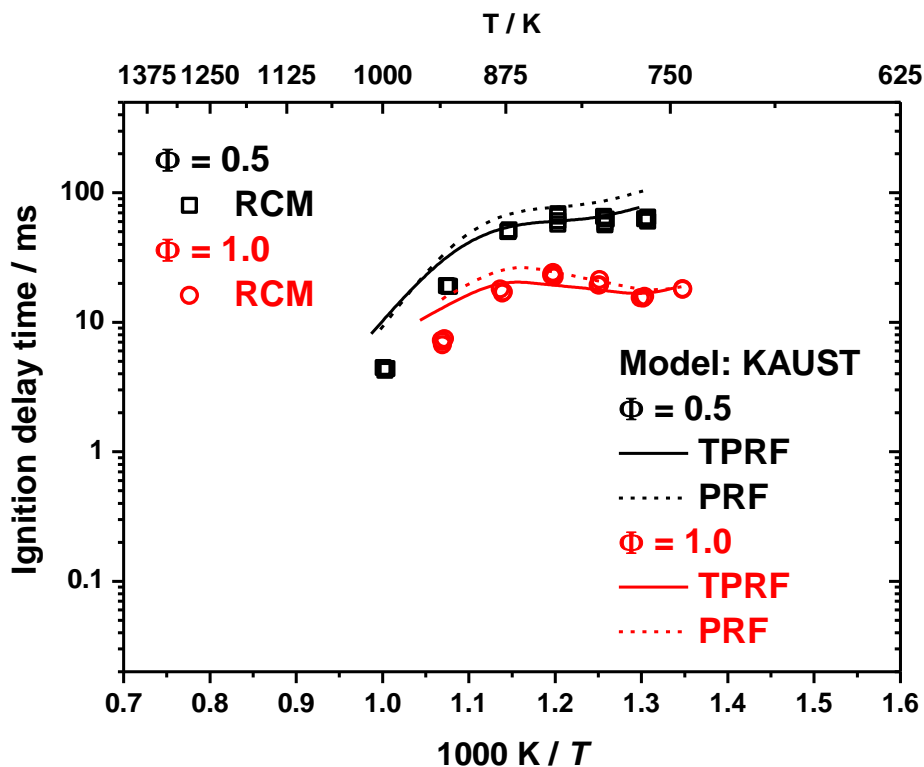


Figure 5. IDT simulation for Coryton gasoline/diesel 50/50 fuel blend using two different gasoline surrogates at  $\phi = 0.5$  and  $1.0$ ,  $p = 10$  atm.

The experimental results show a clear negative temperature coefficient (NTC) behavior in the temperature range 750 to 900 K, it is worth nothing that because of the high initial temperature (150 °C) setting, even by using 100% CO<sub>2</sub> as diluent gas, the lowest compressed gas temperature achieved here is approximately 750 K. The reactivity increases with increasing pressure and equivalence ratio. The divergence becomes more pronounced in the NTC regime, due to an increased concentration of fuel, since fuel radical chemistry dominates the fuel's reactivity in this temperature regime. In general, both gasoline surrogates can capture well the experimental IDTs over a wide range of temperatures, equivalence ratios and pressures. The TPRF surrogate performs better than the PRF surrogate as we expected, and the PRF surrogate shows a more pronounced NTC behavior than the TPRF surrogate.

Moreover, to systematically compare the reactivity of the four different fuels and eliminate the effect of the limited quantity of experimental data presented in Table 2 in addition to facilities effects, constant volume simulations have been performed for these four different fuels, using two different gasoline surrogates and two kinetic models, at three different equivalence ratios and two different pressures. Here, simulation results at  $\phi = 1.0$  and  $p = 10$  atm were selected as representatives, shown

in Figure 6. The reactivity of four different fuels were compared as a function of different gasoline surrogates and kinetic models. At intermediate to high temperatures (900 – 1400 K), all four fuels present the same reactivity, which indicates the dominance of oxygen chemistry over this temperature regime. In the NTC regime (700 – 900 K), IDTs decrease from the fuel with the highest octane number (pure gasoline) to that with the lowest (50/50 gasoline/diesel). Particularly at 750 K, the discrepancy is about a factor of 1.5 – 2.0. This discrepancy corresponds to the experimental data shown in Figure 3. In general, the LLNL model shows a more pronounced NTC behavior than the KAUST model, and the PRF surrogate shows a more pronounced NTC behavior than the TPRF surrogate. It is worth noting that the simulation results of the high RON and high sensitivity fuel (Coryton gasoline) using the TPRF surrogate are unreasonably slow which has been highlighted in Figure 6, this will be further investigated in the next section.

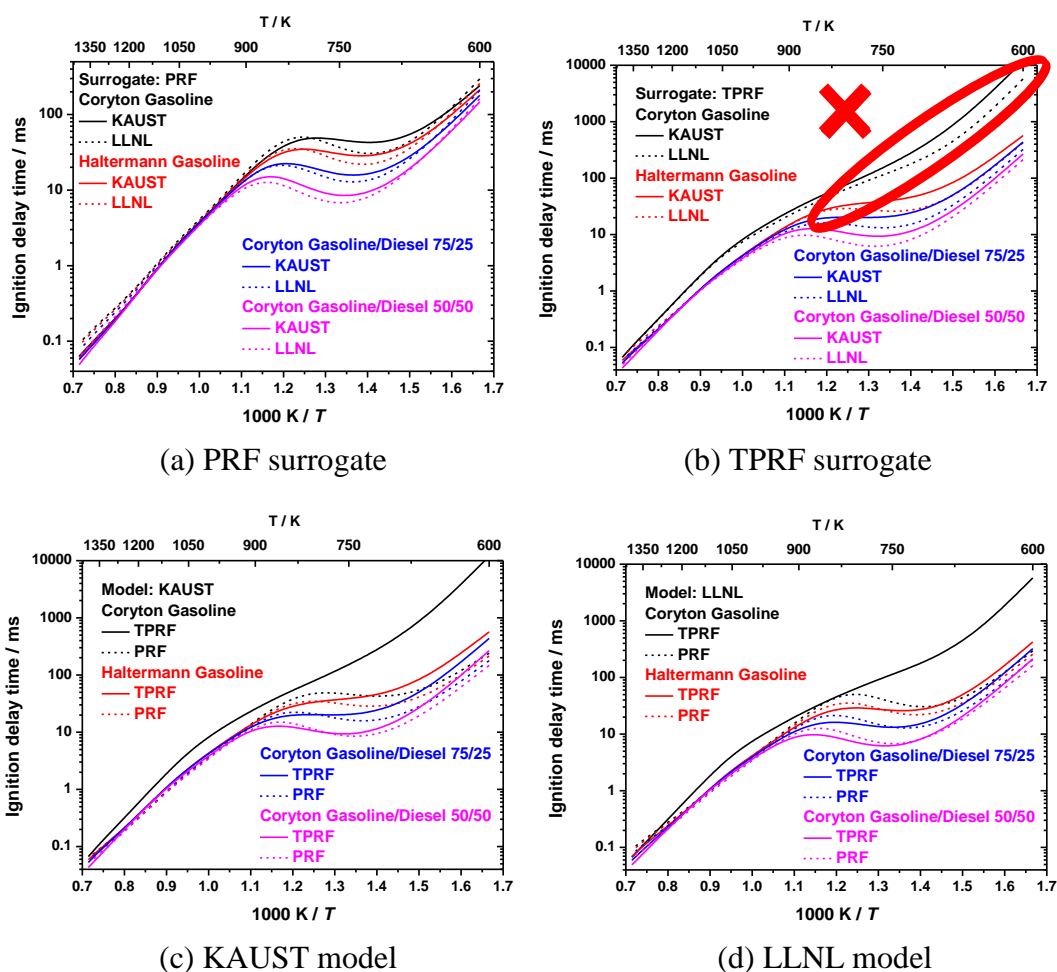


Figure 6. Constant volume IDT simulation for four different fuels at  $\phi = 1.0$  and  $p = 10$  atm.

## 5. TPRF surrogate chemistry

In this section, we aim to investigate the TPRF surrogate chemistry for Coryton gasoline. Given that the IDT of Coryton gasoline was over predicted by TPRF surrogate using the LLNL model [7] and KAUST model [8] (shown in Figure 6), one more recently updated gasoline surrogate model developed from LLNL [14, 15] is used in this section, which has been named as “LLNL\_New”. The major difference between the LLNL and LLNL\_New model is the toluene sub-mechanism, LLNL\_New model has adopted an updated toluene model developed by Zhang et al. [16], which has been well validated. Figure 7 shows the comparison of toluene IDT predictions using four different models (in different colors), it can be seen that Zhang and LLNL\_New models predict identical results, so do LLNL and KAUST models. Meanwhile, the update toluene chemistry shows less reactivity than the old ones.

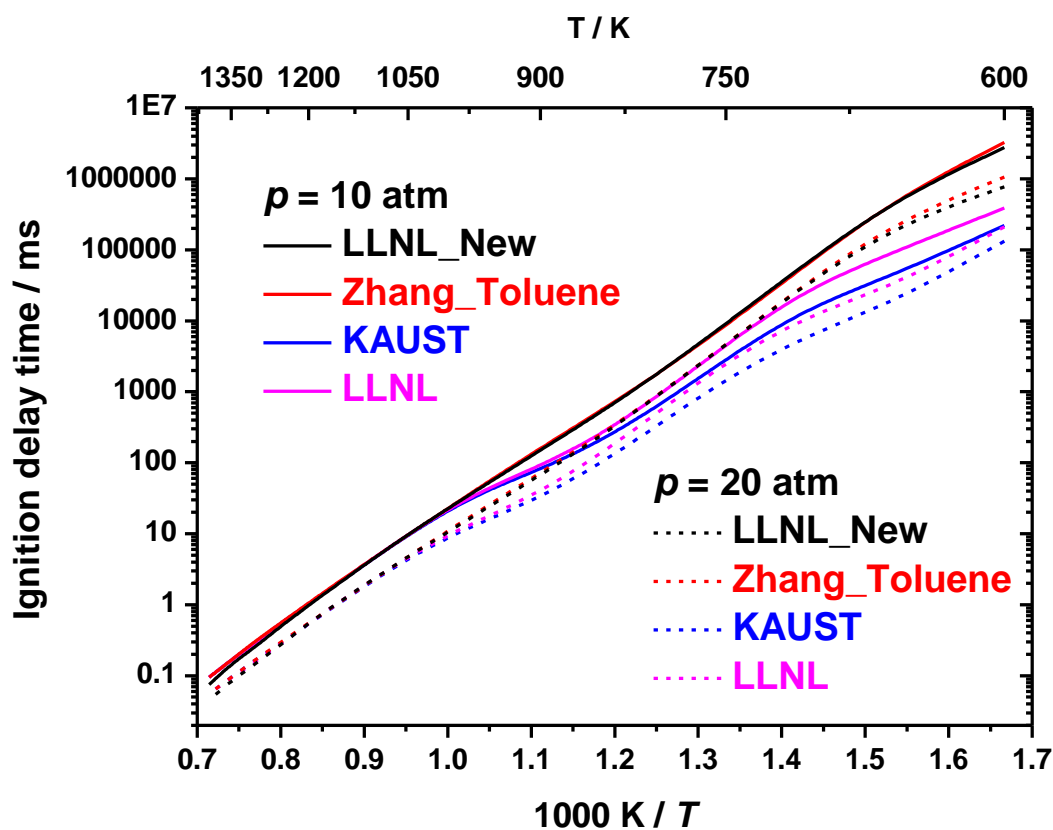


Figure 7. Comparison of toluene IDT predictions using four different models at  $\phi = 1.0$ , and  $p = 10$  and 20 atm.

Figure 8 shows the IDT simulation based on TPRF surrogate for four different fuels using LLNL\_New and KAUST models at  $\phi = 1.0$  and  $p = 10$  atm. For the Coryton gasoline simulation in black color, LLNL\_New model predicts much shorter IDTs than KAUST model towards low

temperature ( $T < 800$  K), indicating a more pronounced NTC behavior. Interestingly, with large quantity of toluene (77.6% by volume) in the TPRF surrogate, such reactivity difference is opposite to that shown in Figure 7. Therefore, a more detailed investigation was carried out including the reactants' concentration profile, flux and sensitivity analyses, all simulation methods and approaches can be found in our recent publications [17, 18].

Figure 9 shows the reactants' concentration and pressure profiles for Coryton gasoline oxidation using TPRF surrogate and LLNL\_New model at  $\phi = 1.0$ ,  $p = 10$  atm and  $T = 750$  K. In the figure, different line colors and types stand for different components and models respectively, and the pressure traces are in magenta color corresponding to the y-axis at right side. A clear two-stage ignition event was observed for simulation using LLNL\_New model, which can be attributed to the low-temperature oxidation chemistry of saturated alkyl radicals from iso-octane and n-heptane.

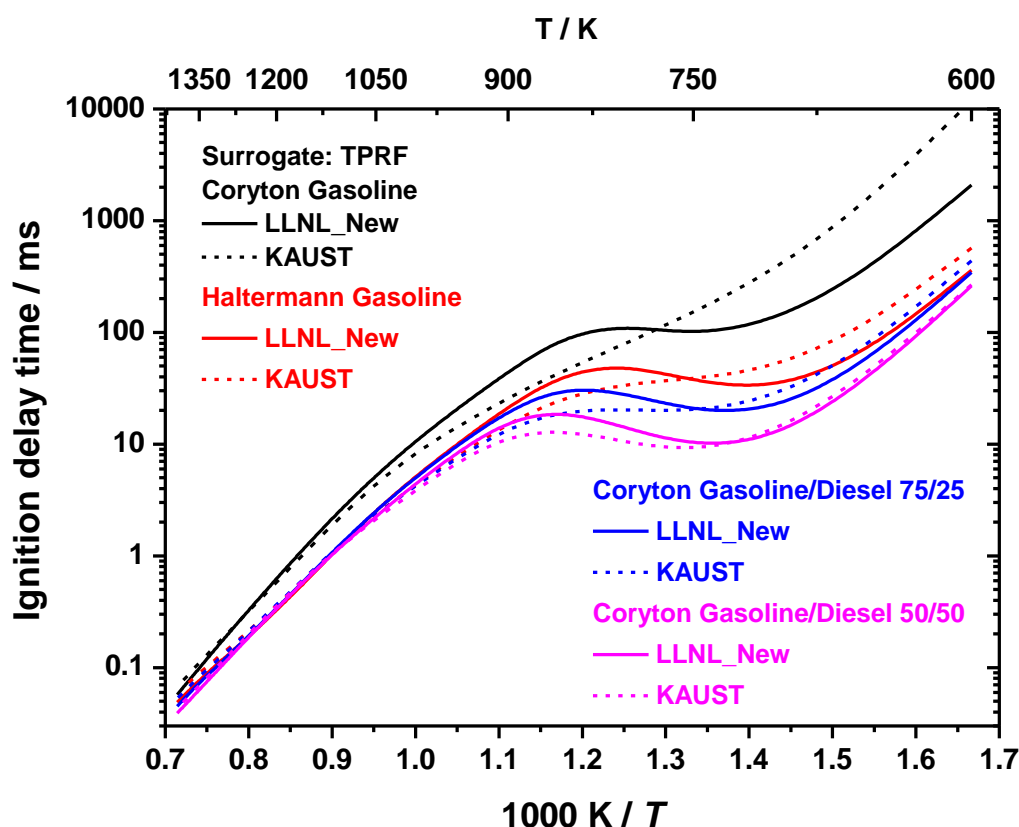


Figure 8. IDT simulation based on TPRF surrogate for four different fuels using LLNL\_New and KAUST models at  $\phi = 1.0$  and  $p = 10$  atm.

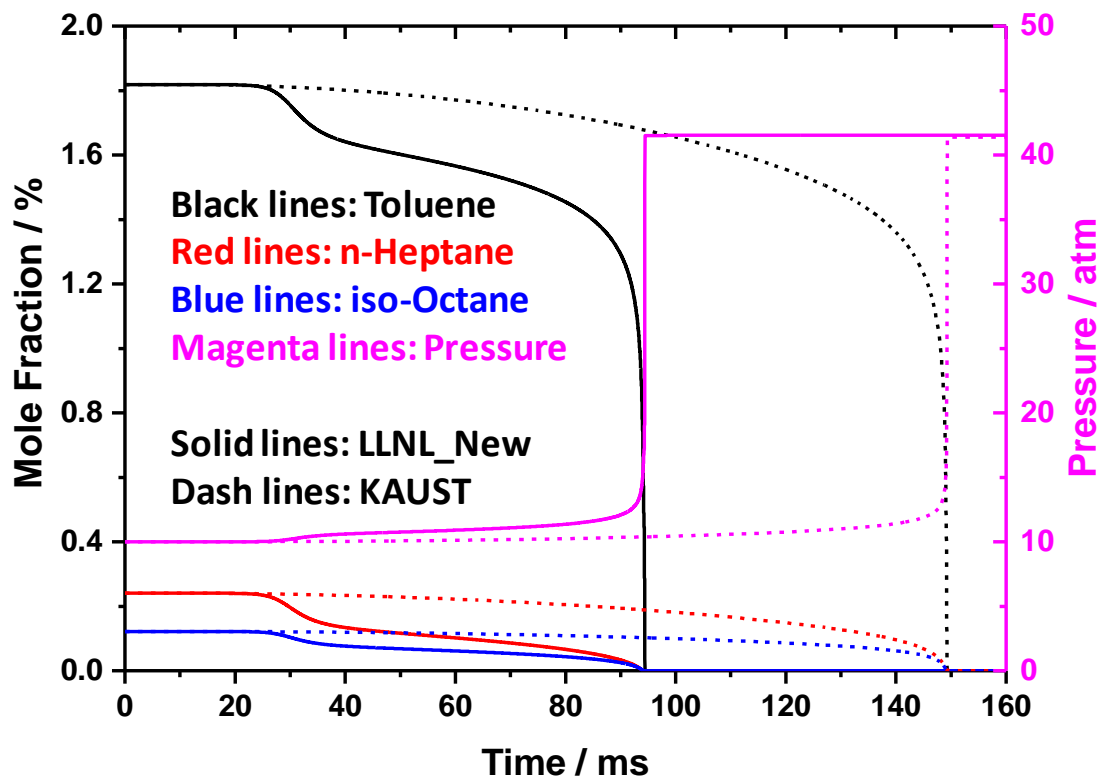


Figure 9. Reactants' concentration and pressure profiles for Coryton gasoline oxidation using TPRF surrogate and LLNL\_New model at  $\phi = 1.0$ ,  $p = 10$  atm and  $T = 750$  K.

Figure 10 shows the flux analysis for the TPRF surrogate blend at  $\phi = 1.0$ ,  $p = 10$  atm,  $T = 750$  K, and at the timing of the rapid decay of reactants after the first stage ignition, which is around 30 ms. In order to make the results more visualized, only the qualitative or generalized reaction pathways were exhibited in the figure, while the quantitative values for the flux of all reactions have been gathered in the Supplementary Material 2. As can be seen, both iso-octane and n-heptane exhibit typical alkyl radical low temperature chemistries, the competition between the  $\dot{\text{H}}\text{O}_2$  radical concerted elimination from  $\text{RO}_2$  and  $\text{RO}_2$  isomerization to  $\text{QOOH}$  leads to the NTC behavior [19, 20].

Figure 11 shows the sensitivity analysis for pure toluene and TPRF surrogate blend at  $\phi = 1.0$ ,  $p = 10$  atm and  $T = 750$  K, it can be seen that, the most inhibiting reaction is the fuel initiation chemistry: H-atom abstraction from the allylic H-atom on the methyl group by  $\dot{\text{O}}\text{H}$  radical forming the benzyl radical ( $\text{C}_6\text{H}_5\text{CH}_2$ ). Thereafter, the reactions between the formed benzyl radical ( $\text{C}_6\text{H}_5\text{CH}_2$ ) and  $\dot{\text{H}}\text{O}_2$  radical on the potential energy surface (PES) of  $\text{C}_6\text{H}_5\text{CH}_2\text{OOH}$  took over the dominance, the association reaction forming benzyl-peroxy (BZCOOH) and chemical activation reaction forming benzyloxy radical ( $\text{C}_6\text{H}_5\text{CH}_2\dot{\text{O}}$ ) plus  $\dot{\text{O}}\text{H}$  radical became the top reactivity inhibiting and promoting

reactions respectively. Of interest is that sensitivity analysis results shows that by mixing toluene into the n-heptane and iso-octane, the main promoting reaction, namely allylic H-atom abstraction by molecular oxygen ( $C_6H_5CH_3 + O_2 \leftrightarrow C_6H_5CH_2 + HO_2$ ) turned into an inhibiting reaction, as highlighted in red rounded rectangles. The flux analysis shows that, this abstraction reaction actually occurs in the reverse direction. To summarize, by blending toluene with PRF,  $HO_2$  radical can be sourced from the concerted elimination reaction of  $RO_2$  radicals from the iso-octane and n-heptane oxidation. Then it reacts with benzyl radical ( $C_6H_5CH_2$ ) via association or chemical activation reactions on the  $C_6H_5CH_2OOH$  PES, or reacts reversely to give initial reactants (toluene and molecular oxygen). With more accurate toluene chemistry, LLNL\_New model was able to predict above complex interaction, which results in more reasonable IDT results as shown in Figure 8.

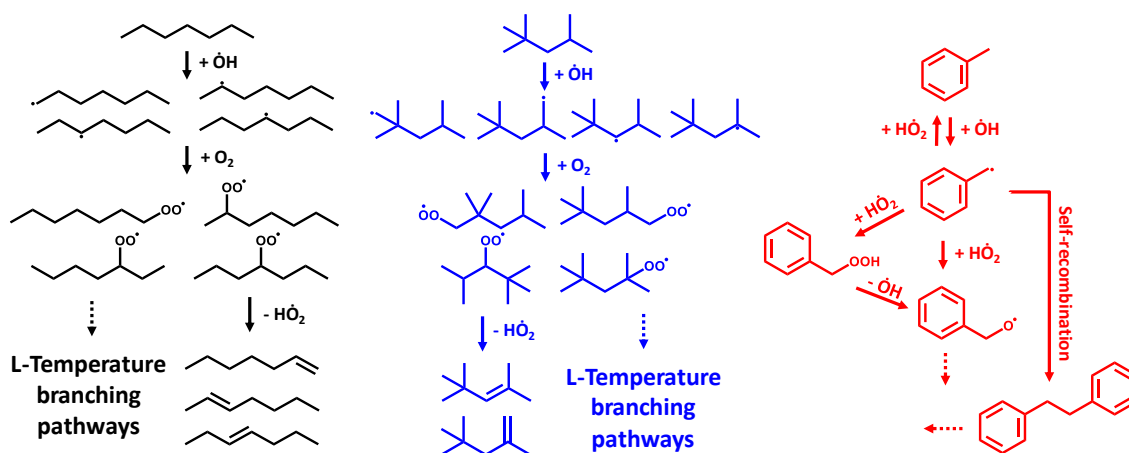


Figure 10. Flux analysis for the TPRF surrogate blend at  $\phi = 1.0$ ,  $p = 10$  atm and  $T = 750$  K.

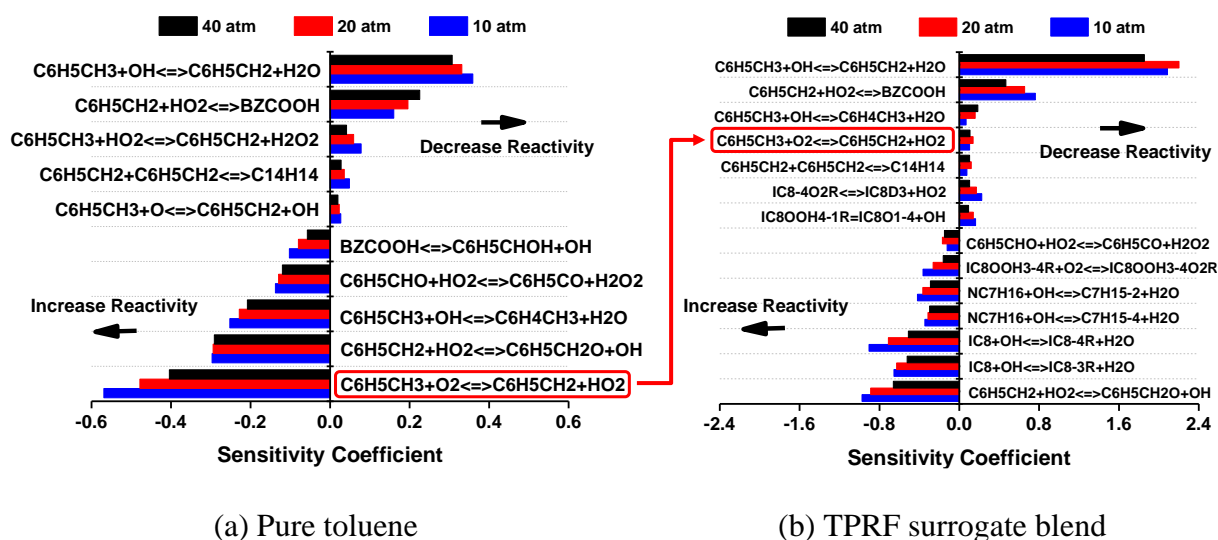


Figure 11. Sensitivity analyses for pure toluene and TPRF surrogate blend at  $\phi = 1.0$ ,  $p = 10$  atm and  $T = 750$  K.

## 6. Conclusions

This work represents an ignition delay study of two Coryton gasoline/diesel fuel blends (75/25 and 50/50) oxidation at elevated pressures in a HPST and in a RCM over a wide range of pressures, temperatures and equivalence ratios. The results presented provide ignition delay time (reactivity) of Coryton gasoline/diesel fuel blends at engine relevant conditions. It was found that increasing pressure resulted in shorter measured ignition delay times (higher reactivity) for all equivalence ratios investigated, which is typical of the influence of pressure on fuel reactivity. The effect of equivalence ratio on ignition delay times depended on the temperature regime of the experiment, whereas all mixtures had similar reactivity at higher temperatures ( $> 900$  K), fuel-rich mixtures are most reactive at lower temperatures ( $< 900$  K). NTC behavior was observed in the low temperature regime (700 – 900 K).

In addition, the reactivity of four different gasoline and diesel fuels: Coryton gasoline, Haltermann gasoline, Coryton gasoline/diesel 75/25 and Coryton gasoline/diesel 50/50 fuel blends were systematically compared under the same experimental conditions. It was found that the lower RON fuel has shorter IDT than that of higher RON fuel, and this phenomenon becomes more pronounced the richer the fuel blend ( $\phi = 2.0$ ), particularly in the NTC regime; at 750 K the discrepancy is about a factor of 1.5 – 2.0.

It was found that TPRF surrogate simulation results for high RON and high octane sensitivity fuel (Coryton gasoline) are unreasonably slow using both LLNL and KAUST models, and this is mainly due to the large quantity of toluene (77.6% by volume) in the surrogate. A detailed investigation was then carried out using a recently published LLNL\_New model which contains an updated toluene sub-mechanism. Reactants' concentration profile, flux and sensitivity analyses were simultaneously performed, from which, toluene chemistry and its interaction with alkane (n-heptane and iso-octane) chemistry were discovered. In toluene oxidation,  $\text{HO}_2$  radical was only involved with the reaction with the benzyl radical ( $\text{C}_6\text{H}_5\text{CH}_2$ ), however, three different reaction types were found to control the reactivity comprehensively: (a) association reaction forming the benzyl-peroxy (BZCOOH); (b)

chemical activation reaction forming the benzoxy radical ( $C_6H_5CH_2\dot{O}$ ) plus  $\dot{O}H$ ; (c) reverse reaction of H-atom abstraction from methyl group by molecular oxygen ( $C_6H_5CH_3 + O_2 \leftrightarrow C_6H_5CH_2 + HO_2$ ).

## Acknowledgements

The authors acknowledge the former colleagues from the Combustion Chemistry Centre of National University of Ireland, Galway and Clean Combustion Research Center of King Abdullah University of Science and Technology for the helpful discussions.

## Supplementary Materials

Supplementary Material 1: Additional information and experimental data

Supplementary Material 2: Flux analysis results

Supplementary Material 3: Volume-time histories of RCM experiments

## References

- [1] W J Pitz, N P Cernansky, F L Drye, et al. Development of an experimental database and chemical kinetic models for surrogate gasoline fuels[C]// SAE International, 2007.
- [2] S M Sarathy, A Farooq, G T Kalghatgi. Recent progress in gasoline surrogate fuels[J]. *Progress in Energy and Combustion Science*, 2018 (65): 67-108.
- [3] G Kalghatgi, Is it really the end of internal combustion engines and petroleum in transport? [J]. *Applied Energy*, 2018 (225): 965-974.
- [4] G Kalghatgi, H Levinsky, M Colket. Future transportation fuels[J]. *Progress in Energy and Combustion Science*, 2018 (69): 103-105.
- [5] G Kukkadapu, C J Sung. Autoignition study of ULSD#2 and FD9A diesel blends[J]. *Combustion and Flame*, 2016 (166): 45-54.
- [6] C Lee, A Ahmed, E F Nasir, et al. Autoignition characteristics of oxygenated gasolines[J]. *Combustion and Flame*, 2017 (186): 114-128.
- [7] M Mehl, J Y Chen, W J Pitz et al. An Approach for Formulating Surrogates for Gasoline with Application toward a Reduced Surrogate Mechanism for CFD Engine Modeling[J]. *Energy & Fuels*, 2011 (25): 5215-5223.
- [8] N Atef, G Kukkadapu, S Y Mohamed et al. A comprehensive iso-octane combustion model with improved thermochemistry and chemical kinetics[J]. *Combustion and Flame* 178 (2017) 111-134.
- [9] Y Li, C W Zhou, H J Curran, An extensive experimental and modeling study of 1-butene oxidation[J]. *Combustion and Flame* 181 (2017) 198-213.
- [10] D2699-19 Standard Test Method for Research Octane Number of Spark-Ignition Engine Fuel[S]. West Conshohocken, PA: ASTM International, doi:[https://doi.org/10.1520/D2699-19\(2019\)](https://doi.org/10.1520/D2699-19(2019)).
- [11] D2700-19 Standard Test Method for Motor Octane Number of Spark-Ignition Engine Fuel[S]. West Conshohocken, PA: ASTM International, doi:[https://doi.org/10.1520/D2700-19\(2019\)](https://doi.org/10.1520/D2700-19(2019)).

- [12] N Morgan, A Smallbone, A Bhave, et al. Mapping surrogate gasoline compositions into RON/MON space[J]. *Combustion and Flame*, 2010 (157):1122-1131.
- [13] G Kalghatgi, H Babiker, J Badra. A simple method to predict knock using toluene, N-Heptane and iso-octane blends (TPRF) as gasoline surrogates[J]. *SAE Int J Engines*, 2015 (8): 505-519.
- [14] M Mehl, S Wagnon, K Tsang, et al. A comprehensive detailed kinetic mechanism for the simulation of transportation fuels[R]. Lawrence Livermore National Lab (LLNL), Livermore, CA, United States, 2017.
- [15] M Mehl, K Zhang, S W Wagnon, et al. A Comprehensive Detailed Kinetic Mechanism for the Simulation of Transportation Fuels[R]. Lawrence Livermore National Lab (LLNL), Livermore, CA, United States, 2018.
- [16] Y Zhang, H El-Merhubi, B Lefort et al. Probing the low-temperature chemistry of ethanol via the addition of dimethyl ether[J]. *Combustion and Flame*, 2018 (190) :74-86.
- [17] C W Zhou, Y Li, E O'Connor et al., A comprehensive experimental and modeling study of isobutene oxidation[J]. *Combustion and Flame*, 2016 (167): 353-379.
- [18] C W Zhou, Y Li, U Burke et al., An experimental and chemical kinetic modeling study of 1,3-butadiene combustion: Ignition delay time and laminar flame speed measurements[J]. *Combustion and Flame*, 2018 (197): 423-438.
- [19] K Zhang, C Banyon, J Bugler et al. An updated experimental and kinetic modeling study of n-heptane oxidation[J]. *Combustion and Flame*, 2016 (172):116-135.
- [20] N Atef, G Kukkadapu, S Y Mohamed et al. A comprehensive iso-octane combustion model with improved thermochemistry and chemical kinetics, *Combustion and Flame* 178 (2017) 111-134.